Deep Multiomics Profiling of Brain Tumors Identifies Signaling Networks Downstream of Cancer Driver Genes

Wang et al

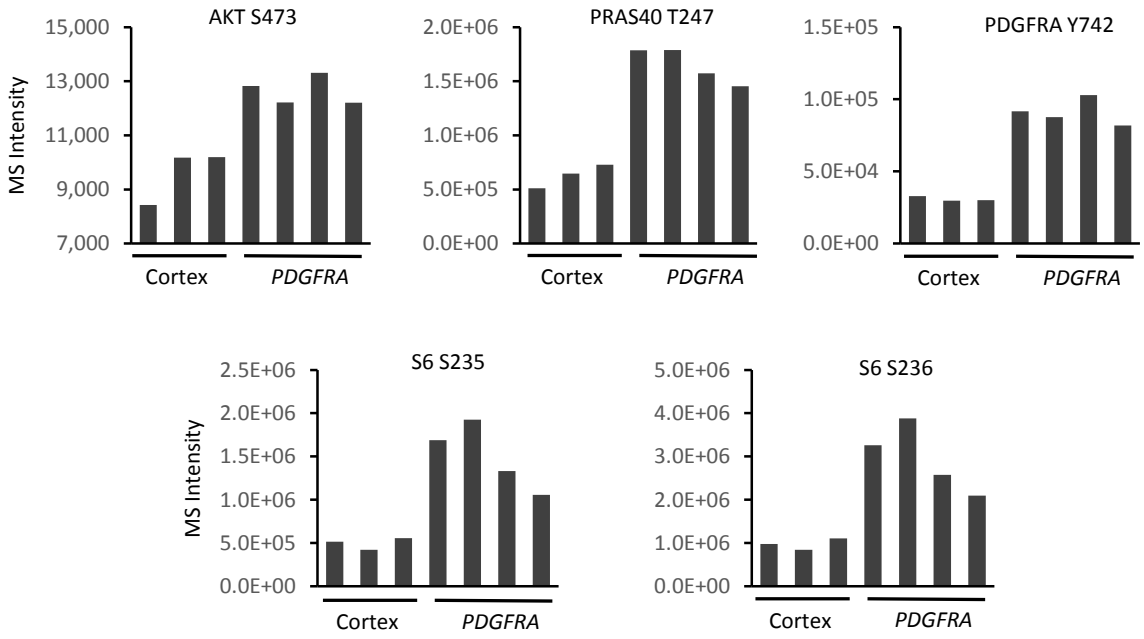

Supplementary Figure 1 | MS-based quantification is accurate

MS measurements of phosphorylation events are highly consistent with previous immunoblot assays comparing *PDGFRA*-driven HGGs to normal cortex (Paugh BS *et al*. 2013).

a Standard deviation matrix of pairwise sample comparison (Log_2) in whole proteome and phosphoproteome

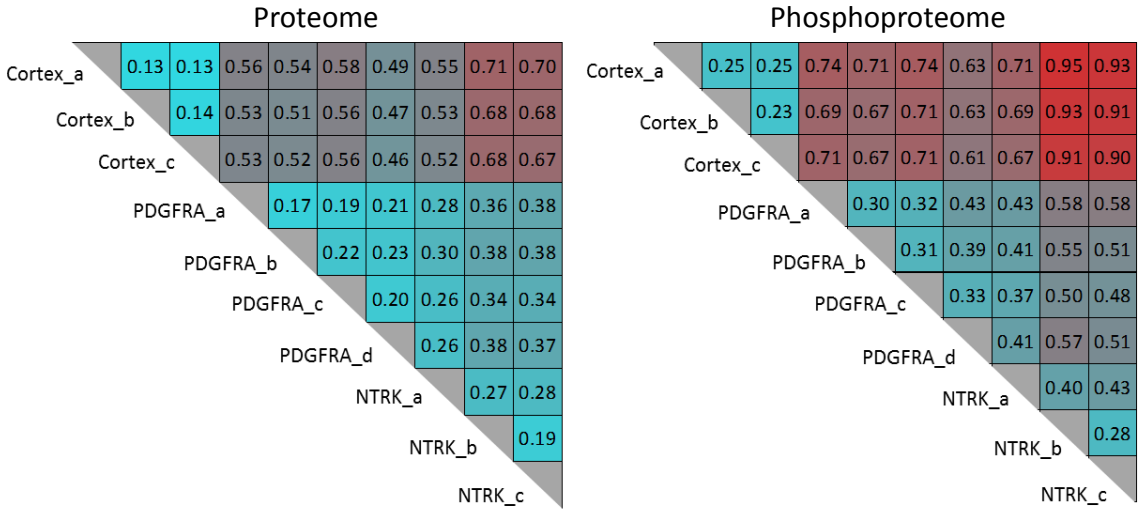

b

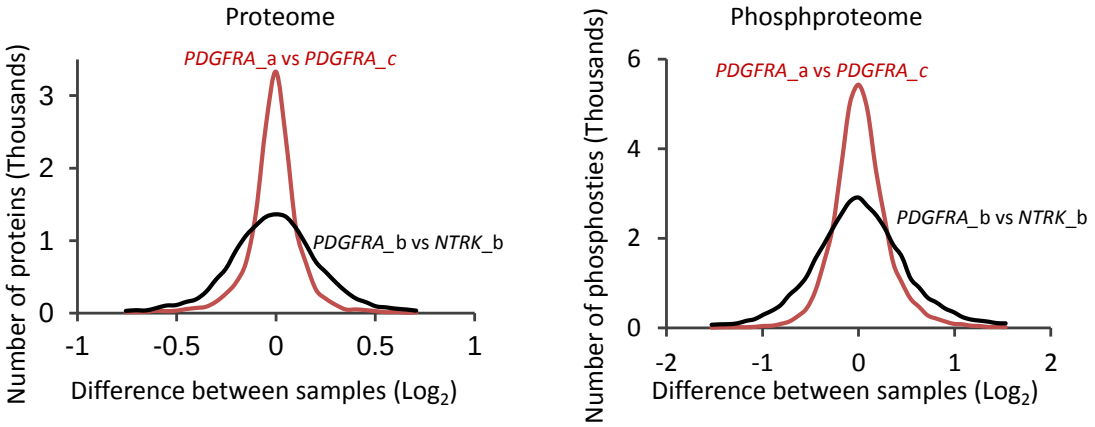

Supplementary Figure 2 | MS-based proteomic analyses specify particularly small variations

(a) Pairwise standard deviation matrix of whole proteome and phosphoproteome displays particularly small variations between replicates.

(b) Examples show distributions of representative Log_2 level whole proteome and phosphoproteome variations between *PDGFRA*-driven HGG biological replicates and between two HGG tumors.

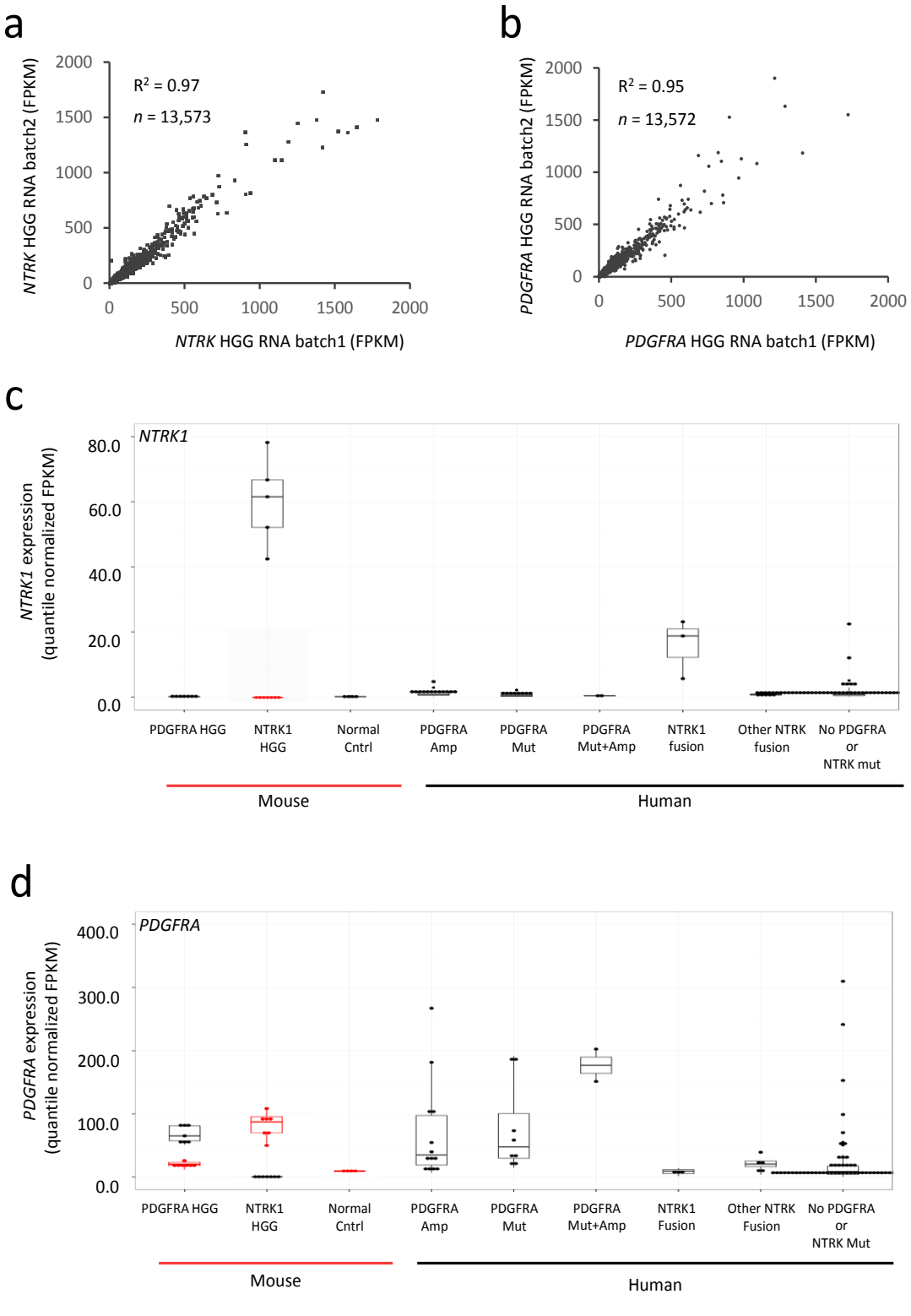
a
NTRK HGG RNA batch2 (FPKM)
R² = 0.97
n = 13,573
NTRK HGG RNA batch1 (FPKM)
b
PDGFRA HGG RNA batch2 (FPKM)
R² = 0.95
n = 13,572
PDGFRA HGG RNA batch1 (FPKM)
c
NTRK1
NTRK1 expression (quantile normalized FPKM)
PDGFRA HGG
NTRK1 HGG
Normal Cntrl
PDGFRA Amp
PDGFRA Mut
PDGFRA Mut+Amp
NTRK1 fusion
Other NTRK fusion
No PDGFRA or NTRK mut
Mouse
Human
d
PDGFRA
PDGFRA expression (quantile normalized FPKM)
PDGFRA HGG
NTRK1 HGG
Normal Cntrl
PDGFRA Amp
PDGFRA Mut
PDGFRA Mut+Amp
NTRK1 Fusion
Other NTRK Fusion
No PDGFRA or NTRK Mut
Mouse
Human

Supplementary Figure 3 | HGG mouse models are reproducible

(a, b) Comparisons of RNAseq results on batch2 and batch1 HGG mouse models show highly consistent transcript abundance from tumors generated by independent experiments. Scatterplots show FPKM values of genes in batch1 and batch2 HGG mouse models, Pearson correlations were performed and R^2 values were shown on the upper left side of the panels.

(c, d) Mouse tumors express levels of mutated PDGFRA or NTRK fusion genes that are relevant to the levels expressed in primary human tumors. Normalized RNAseq data was used to compare the expression of the human NTRK1 (c) or PDGFRA (d) expression in mouse HGGs, control mouse cortex, or human HGGs from Wu et al, Nat Genet, 2014, categorized as HGGs carrying amplified wild-type PDGFRA, mutated PDGFRA, amplified and mutated PDGFRA, TPM3-TRK1 fusion gene, fusion genes involving NTRK2 or 3, or HGGs without mutation in PDGFRA or NTRK genes. Expression of mouse orthologs for NTRK1 (c) or PDGFRA (d) are shown in red. Analysis of variant allele frequency from whole genome sequencing data showed that human tumors with TPM3-NTRK1 fusion gene carried the fusion gene as a subclonal population comprising only 9-20% of the tumor cells. Therefore, expression of the TPM3-NTRK1 from bulk tumor RNA is a significant underestimate of expression of the TPM3-NTRK1 fusion in human tumor cells. Boxplot center line, median; box limits, upper and lower quartiles; whiskers, 1.5x interquartile range; points, outliers.

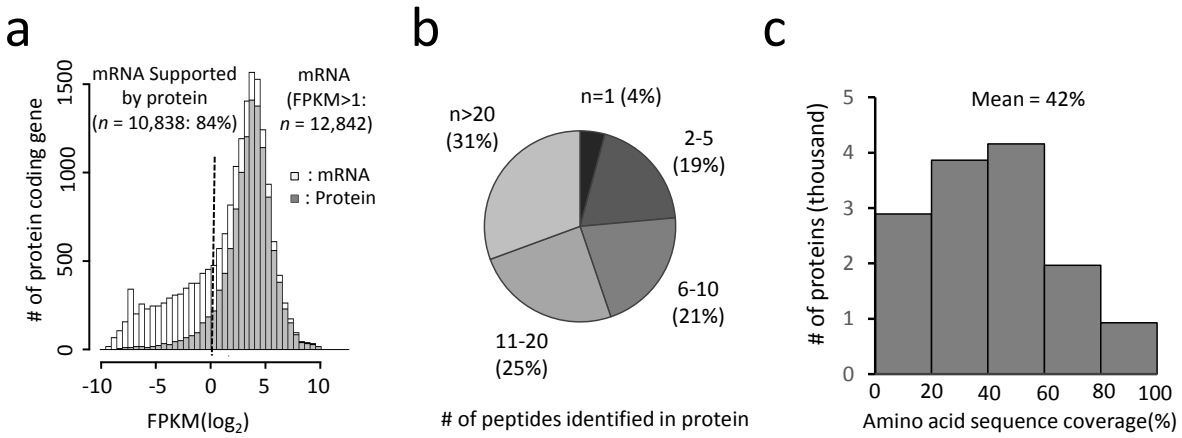

Supplementary Figure 4 | Proteome-transcriptome comparison shows deep proteomic coverage

(a) High percentage (84%) of expressed transcripts detected by MS. In the histogram of transcript log_2FPKM, MS-detected proteins are highlighted in grey. To ensure data stringency, FPKM >1 were applied in this analysis.

(b) The number of peptides identified for each protein in this MS analysis. > 96% of proteins were identified by at least 2 distinct peptides.

(c) The MS coverage of theoretically observable amino acid sequences in a histogram. In average, 42% of observable amino acid sequences were detected in this MS study.

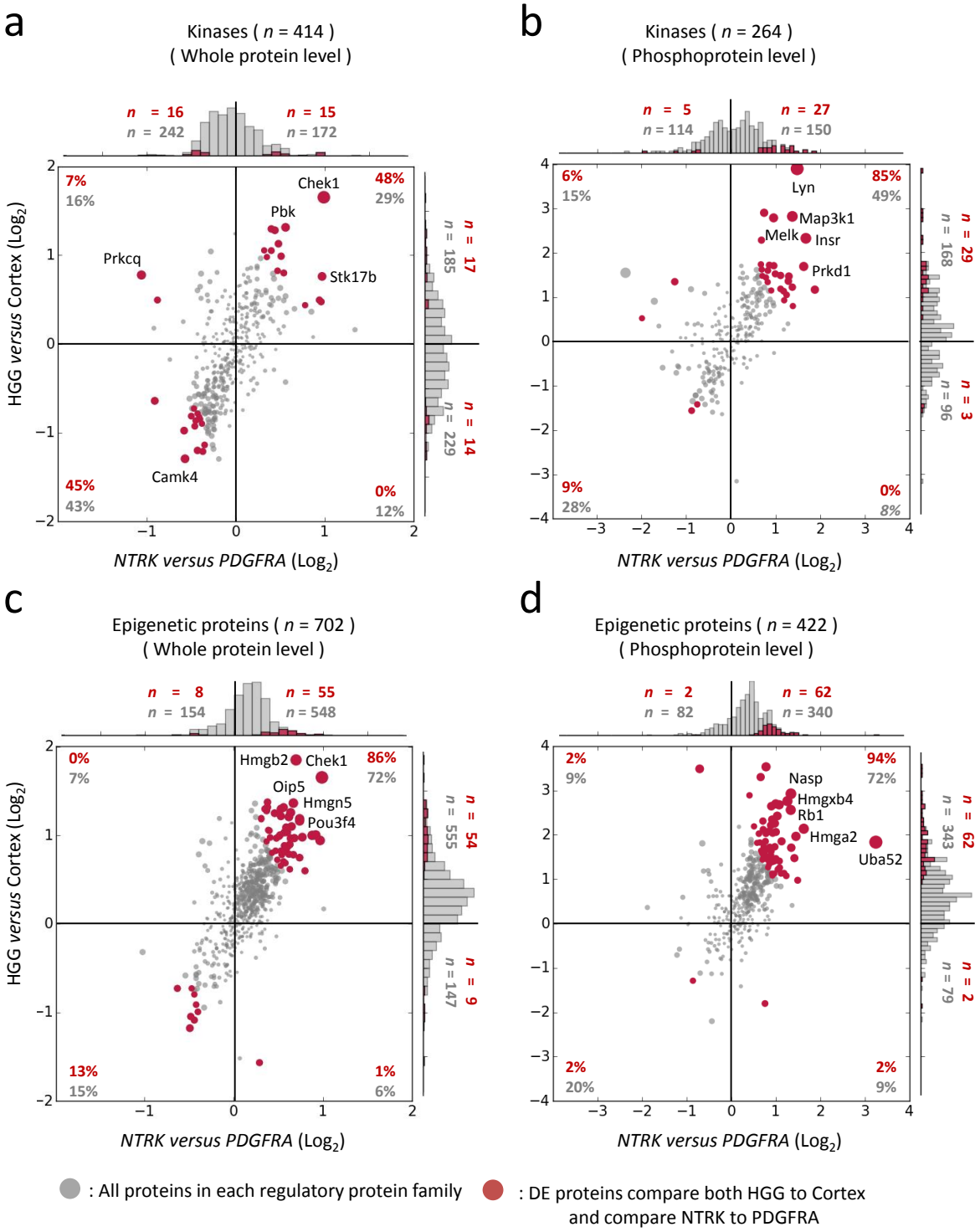
a
Kinases (n = 414)
(Whole protein level)
n = 16
n = 242
n = 15
n = 172
7%
16%
48%
29%
45%
43%
0%
12%
Chek1
Pbk
Prkcq
Stk17b
Camk4
n = 17
n = 185
n = 14
n = 229
HGG versus Cortex (Log2)
NTRK versus PDGFRA (Log2)
b
Kinases (n = 264)
(Phosphoprotein level)
n = 5
n = 114
n = 27
n = 150
6%
15%
85%
49%
9%
28%
0%
8%
Lyn
Map3k1
Melk
Insr
Prkd1
n = 29
n = 168
n = 3
n = 96
NTRK versus PDGFRA (Log2)
c
Epigenetic proteins (n = 702)
(Whole protein level)
n = 8
n = 154
n = 55
n = 548
0%
7%
86%
72%
13%
15%
1%
6%
Hmgb2
Chek1
Oip5
Hmgn5
Pou3f4
n = 54
n = 555
n = 9
n = 147
HGG versus Cortex (Log2)
NTRK versus PDGFRA (Log2)
d
Epigenetic proteins (n = 422)
(Phosphoprotein level)
n = 2
n = 82
n = 62
n = 340
2%
9%
94%
72%
2%
20%
2%
9%
Nasp
Hmgxb4
Rb1
Hmga2
Uba52
n = 62
n = 343
n = 2
n = 79
NTRK versus PDGFRA (Log2)
: All proteins in each regulatory protein family
: DE proteins compare both HGG to Cortex
and compare NTRK to PDGFRA

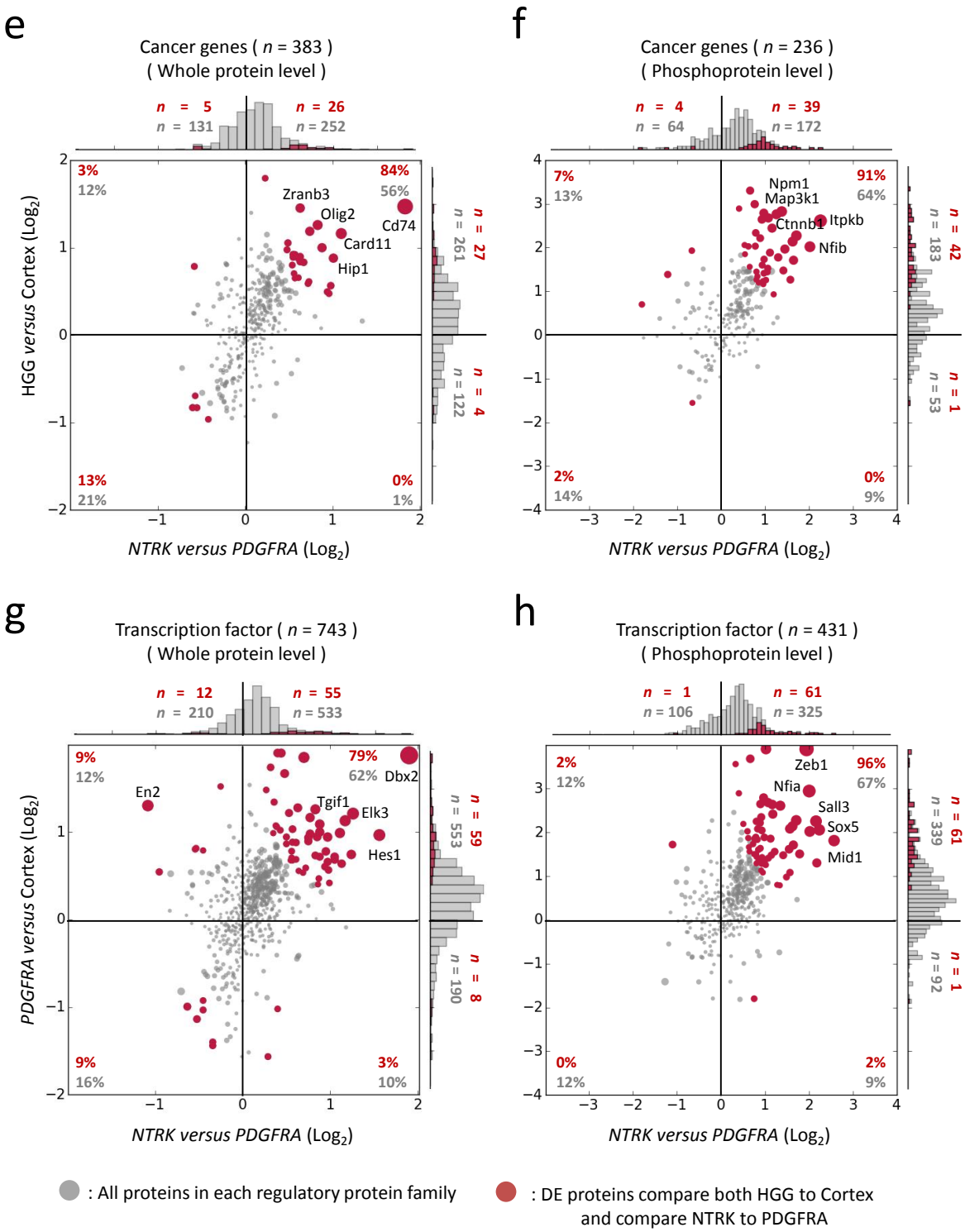
e
Cancer genes (n = 383)
(Whole protein level)
n = 5
n = 131
n = 26
n = 252
3%
12%
84%
56%
Zranb3
Olig2
Cd74
Card11
Hip1
n = 27
n = 261
n = 4
n = 122
13%
21%
0%
1%
HGG versus Cortex (Log2)
NTRK versus PDGFRA (Log2)
f
Cancer genes (n = 236)
(Phosphoprotein level)
n = 4
n = 64
n = 39
n = 172
7%
13%
91%
64%
Npm1
Map3k1
Ctnnb1
Itpkb
Nfib
n = 42
n = 183
n = 1
n = 53
2%
14%
0%
9%
NTRK versus PDGFRA (Log2)
g
Transcription factor (n = 743)
(Whole protein level)
n = 12
n = 210
n = 55
n = 533
9%
12%
79%
62%
Dbx2
En2
Tgif1
Elk3
Hes1
n = 59
n = 553
n = 8
n = 190
9%
16%
3%
10%
PDGFRA versus Cortex (Log2)
NTRK versus PDGFRA (Log2)
h
Transcription factor (n = 431)
(Phosphoprotein level)
n = 1
n = 106
n = 61
n = 325
2%
12%
96%
67%
Zeb1
Nfia
Sall3
Sox5
Mid1
n = 61
n = 339
n = 1
n = 92
0%
12%
2%
9%
NTRK versus PDGFRA (Log2)
: All proteins in each regulatory protein family
: DE proteins compare both HGG to Cortex
and compare NTRK to PDGFRA

Supplementary Figure 5 | Proteomic analyses detect a global trend of increased expression and phosphorylation of regulatory protein families in HGG tumors

(a - h) Deep proteomic data analyses show a global increase of protein expression and phosphorylation of most of regulatory protein families (Kinase, epigenetic genes, transcription factors and cancer genes) in HGG tumors compare to cortex, with higher magnitude of increase in *NTRK*-driven HGG than *PDGFRA*-driven HGG. Scatter-histogram graphs of regulatory family proteins expression and phosphorylation comparing both HGG tumors to cortex and *NTRK*-driven HGGs to *PDGFRA*-driven HGGs. B.H. adjusted Student T test *p* values of 0.05 in both pairwise comparisons plus fold change (FC) cutoff of $FC_{(NTRK/PDGFRA)} * FC_{(HGG/cortex)} > 1.5^2$ for proteome and >2 for phosphoproteome are applied for differential expression analyses. DE genes are shown in red. Magnitude of change is represented by dot size. Top five altered proteins and phosphoproteins with the largest magnitude of alterations are labeled. The distributions of pairwise differences are shown by histograms.

a

Global kinome family rewiring based on substrate-derived kinase activity:
(*NTRK* HGG vs *cortex*)

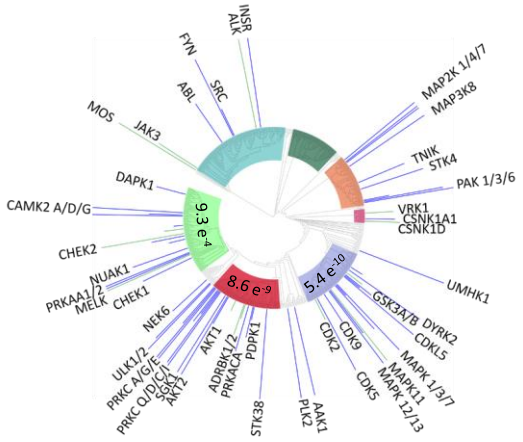

b

Global kinome family rewiring based on substrate-derived kinase activity:
(*PDGFRA HGG* vs *cortex*)

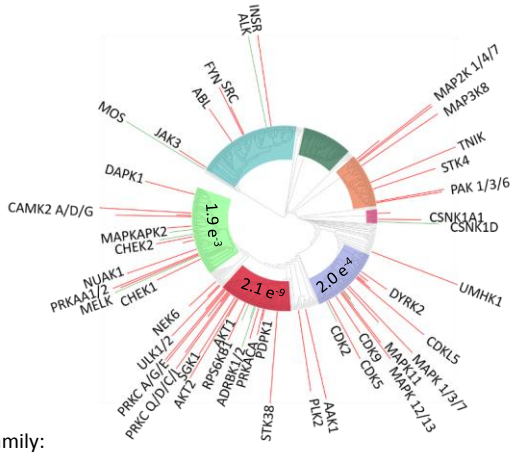

Kinase family:

AGC CAMK CMGC CK1 TK STE

TKL *NTRK* (blue bar), *PDGFRA* (red bar), Cortex (green bar)

Supplementary Figure 6 | AGC, CAMK and CMGC kinase superfamilies display higher activity in both HGG tumors compare to cortex

(a) Kinome tree circular map shows kinase activity comparing *NTRK*-driven HGG to cortex. Pairwise comparisons of kinase superfamilies with a Chi-square *P* values < 0.05 are labelled. Magnitude of kinase activity difference is represented by length of bars located outside of the kinome tree circles. Blue bar indicates higher activity in *NTRK*-driven HGG compare to Cortex. Green bar indicates higher activity in cortex compare to *NTRK*-driven HGG

(b) Kinome tree circular map shows kinase activity comparing *PDGFRA*-driven HGG to cortex. Pairwise comparisons of kinase superfamilies with a Chi-square *P* values < 0.05 are labelled. Magnitude of kinase activity difference is represented by length of bars located outside of the kinome tree circles. Red bar indicates higher activity in *PDGFRA*-driven HGG compare to Cortex. Green bar indicates higher activity in cortex compare to *PDGFRA*-driven HGG

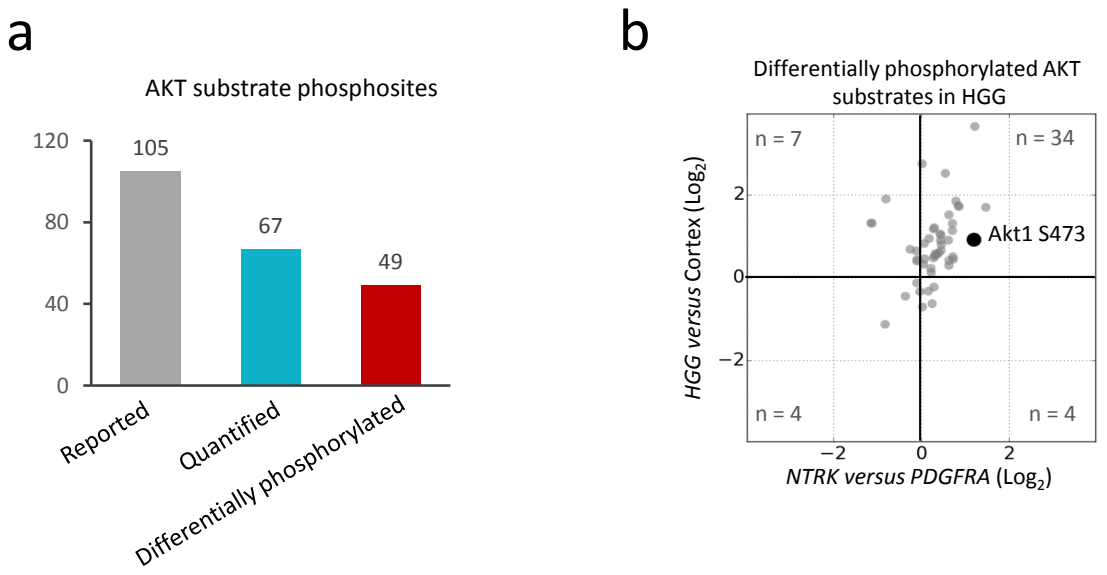

Supplementary Figure 7| Evaluation of AKT regulated substrates

(a) A high percentage of known AKT substrate sites were identified in the deep phosphoproteome. Bar graph shows reported substrate sites, quantified phosphosites and differentially phosphorylated sites.

(b) Differentially phosphorylated substrates that are regulated by AKT in HGGs. Scatter plot of log_2 level changes compare HGG tumors to cortex and compare *NTRK*-driven HGG to *PDGFRA*-driven HGG. Substrates with the same phosphorylation pattern as the AKT active site (S473, located at upper right) were accepted as AKT regulated substrates.

PRKAA1 active substrates

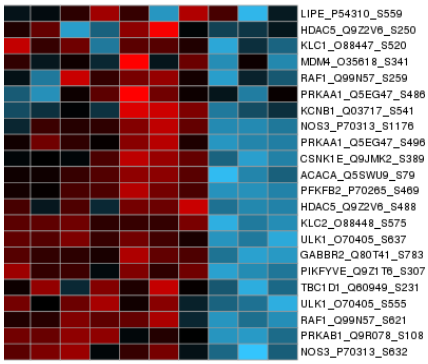

CDK5 active substrates

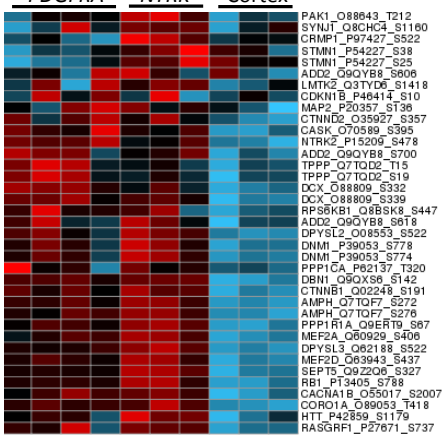

MAPK3 active substrates

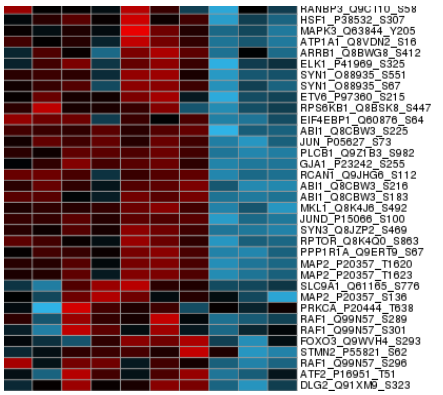

ATR active substrates

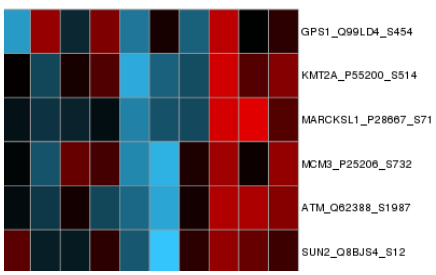

ATM active substrates

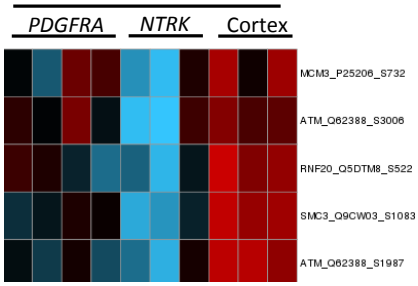

PAK1 active substrates

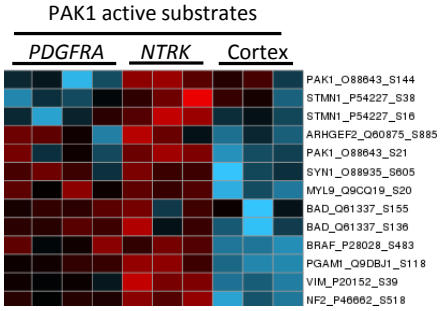

FYN active substrates

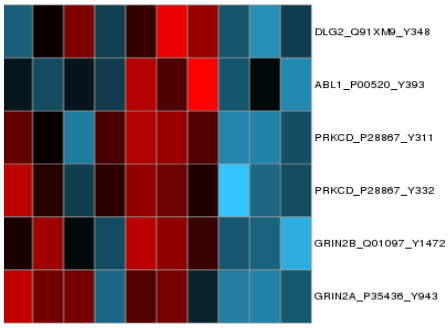

Supplementary Figure 8 | Heatmaps display differentially phosphorylated substrates (with up-regulated phosphorylation in HGG tumors) of other active kinases derived from kinase-substrate analysis. Color key presents the Z score of kinase substrates

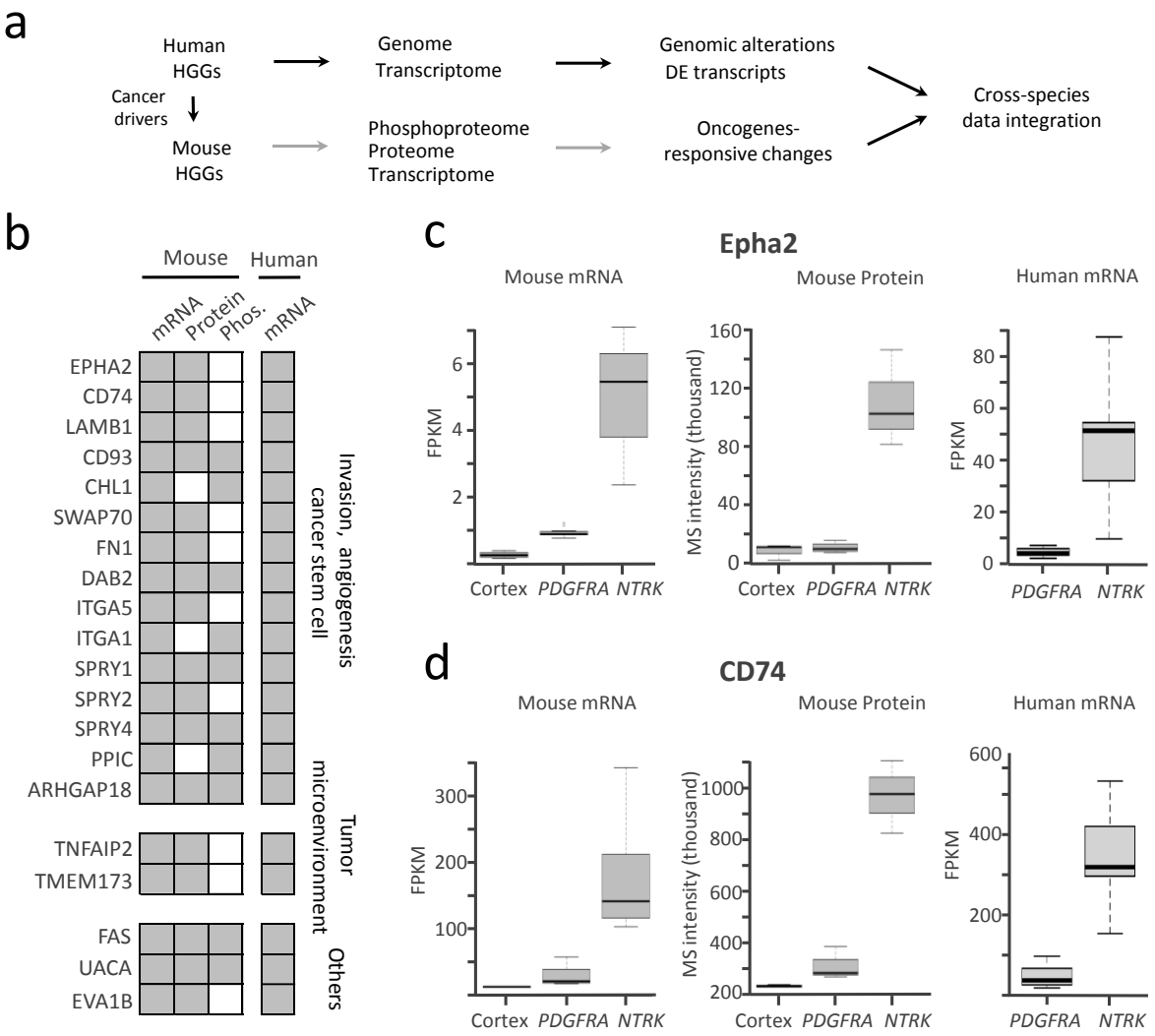
a
Human HGGs
Cancer drivers
Mouse HGGs
Genome
Transcriptome
Phosphoproteome
Proteome
Transcriptome
Genomic alterations
DE transcripts
Oncogenes-responsive changes
Cross-species data integration
b
Mouse
Human
mRNA
Protein
Phos.
mRNA
EPHA2
CD74
LAMB1
CD93
CHL1
SWAP70
FN1
DAB2
ITGA5
ITGA1
SPRY1
SPRY2
SPRY4
PPIC
ARHGAP18
TNFAIP2
TMEM173
FAS
UACA
EVA1B
Invasion, angiogenesis cancer stem cell
Tumor microenvironment
Others
c
Epha2
Mouse mRNA
Mouse Protein
Human mRNA
FPKM
MS intensity (thousand)
Cortex
PDGFRA
NTRK
d
CD74
Mouse mRNA
Mouse Protein
Human mRNA
FPKM
MS intensity (thousand)
Cortex
PDGFRA
NTRK

Supplementary Figure 9 | Combination of mouse and human HGG data prioritizes putative cancer genes.

(a) Overview of multiomics analysis across species

(b) Cross species integrative analysis reveal cancer driver responsive genes, many of which are well-reported cancer genes in HGG. The cancer driver responsive genes were classified according to their functions. Mouse transcripts and proteins/phosphorylations that follow the expression order of *NTRK* > *PDGFRA* > Cortex were accepted to be oncogene responsive. Human transcripts that show *NTRK* > *PDGFRA* were intersected with mouse oncogene responsive genes for prioritization. Gray fills indicate consistent changes identified, while white boxes indicate no significant change or data not available.

(c, d) Boxplots show Epha2 and CD74 expression in multiomics data in human and mouse. Human mRNA boxplots compare expression levels of EPHA2 or CD74 in pediatric HGGs with mutated PDGFRA or NTRK fusion genes. Boxplot center line, median; box limits, upper and lower quartiles; whiskers, 1.5x interquartile range.

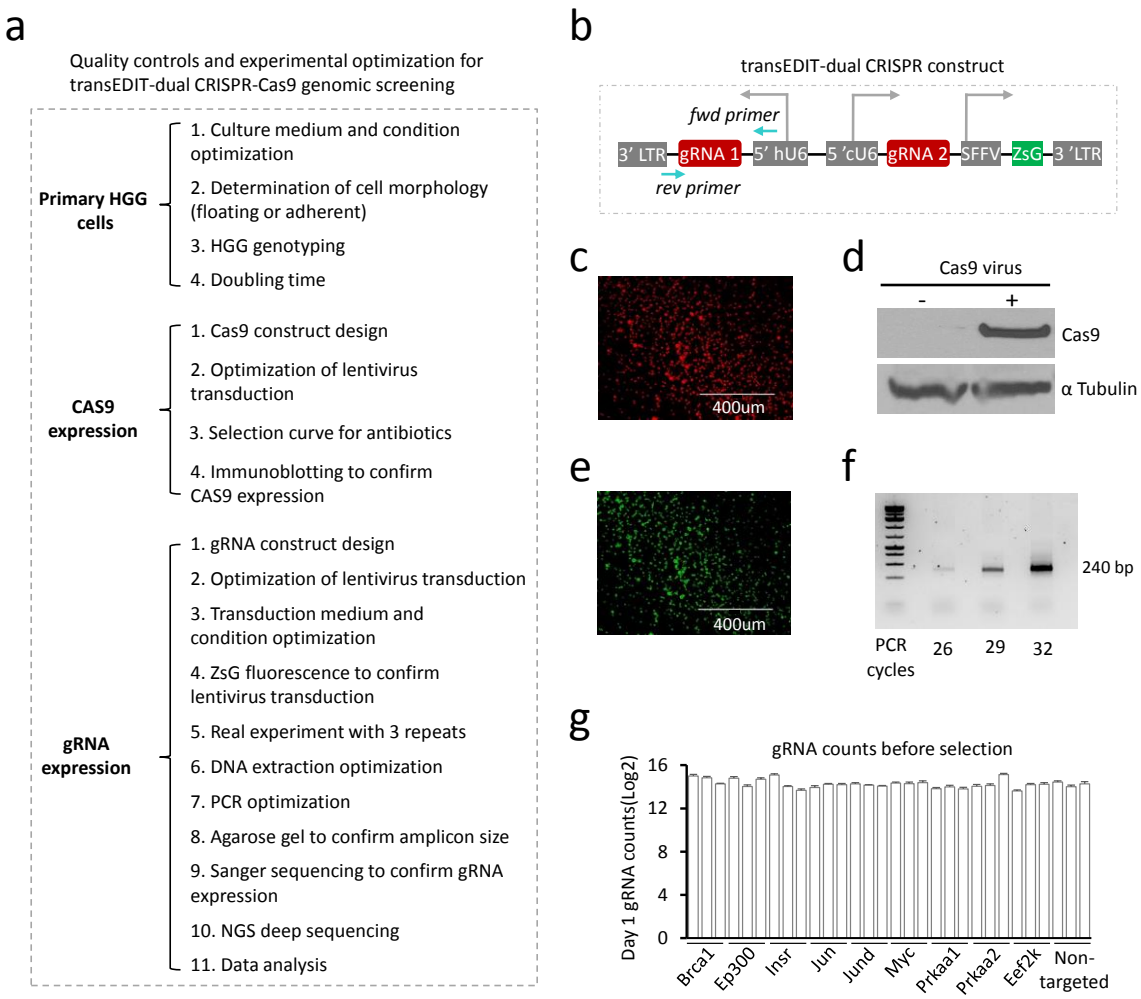
a
Quality controls and experimental optimization for transEDIT-dual CRISPR-Cas9 genomic screening
Primary HGG cells
1. Culture medium and condition optimization
2. Determination of cell morphology (floating or adherent)
3. HGG genotyping
4. Doubling time
CAS9 expression
1. Cas9 construct design
2. Optimization of lentivirus transduction
3. Selection curve for antibiotics
4. Immunoblotting to confirm CAS9 expression
gRNA expression
1. gRNA construct design
2. Optimization of lentivirus transduction
3. Transduction medium and condition optimization
4. ZsG fluorescence to confirm lentivirus transduction
5. Real experiment with 3 repeats
6. DNA extraction optimization
7. PCR optimization
8. Agarose gel to confirm amplicon size
9. Sanger sequencing to confirm gRNA expression
10. NGS deep sequencing
11. Data analysis
b
transEDIT-dual CRISPR construct
fwd primer
3' LTR
gRNA 1
5' hU6
5 'cU6
gRNA 2
SFFV
ZsG
3 'LTR
rev primer
c
400um
d
Cas9 virus
-
+
Cas9
α Tubulin
e
400um
f
240 bp
PCR cycles
26
29
32
g
gRNA counts before selection
Day 1 gRNA counts(Log2)
16
12
8
4
0
Brca1
Ep300
Insr
Jun
Jund
Myc
Prkaa1
Prkaa2
Eef2k
Non-targeted

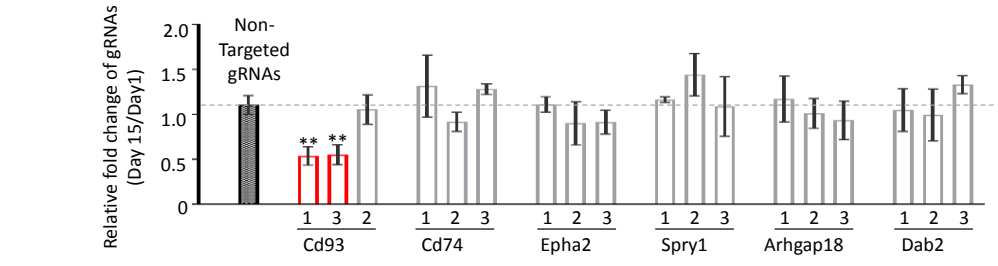
h
Genomic functional screening using customized mini-gRNA library targeting cross-species conserved regulators
Relative fold change of gRNAs (Day 15/Day1)
2.0
1.5
1.0
0.5
0
Non-Targeted gRNAs
**
**
1 3 2
Cd93
1 2 3
Cd74
1 2 3
Epha2
1 2 3
Spry1
1 2 3
Arhgap18
1 2 3
Dab2

Supplementary Figure 10 | Quality controls for CRISPR-CAS9 functional genomic screening using transEDIT-dual system

(a) Work flow and QC steps for CRISPR-Cas9 functional genomic screening using transEDIT-dual system

(b) Simplified cartoon shows transEDIT-dual CRISPR construct with primer binding sites. Two gRNAs targeting different regions of the same genes were designed in a signal CRISPR construct. Primer binding sites for PCR amplification of gRNA 1 were shown. Fwd: forward; rev: Reverse.

(c) Image of primary HGG cells show mCherry fluorescence which co-express with *TPM3-NTRK1* cancer driver gene

(d) Stable expression of Cas9 in HGG cells as validated by immunoblot assay.

(e) gRNA integration was validated by fluorescence detection of ZsG. Image shows the detection of ZsG fluorescence in the primary HGG cells 3 days of transEDIT-dual gRNA lentivirus transduction.

(f) PCR products show amplicon size and band intensities corresponding to different PCR cycle. Theoretical amplicon size is 240bp. PCR cycle 29 was used for later analysis.

(g) Close to even distribution of gRNA counts before selection. Bar plot shows the Log2 level counts of each gRNA collected at 1 day after gRNA transduction. 3 x dual gRNAs were designed for each target gene, and the CRISPR-Cas9 experiment was repeated 3 times. Error bars indicate the s.e.m of 3 experiments.

(h) CRISPR-CAS9 genomic screening targeting top candidate targets derived through cross-species data integration. Bar pot shows the log2 level gRNA relative fold changes of top cross-species conserved regulators after selection for 15 days. Dash line indicates the mean level of all non-targeted gRNA controls. The gRNA counts of cross-species conserved regulators were compared with non-targeted gRNA controls, and red bars indicate gRNA changes that show statistical significance with a Student t test P value smaller than 0.05. Two asterisks: $p < 0.01$.

Fold change distribution and Z-value transformed distribution of MS2 and MS3 based peptide quantification comparing *NTRK-d*riven HGG to Cortex using TMT labeling.

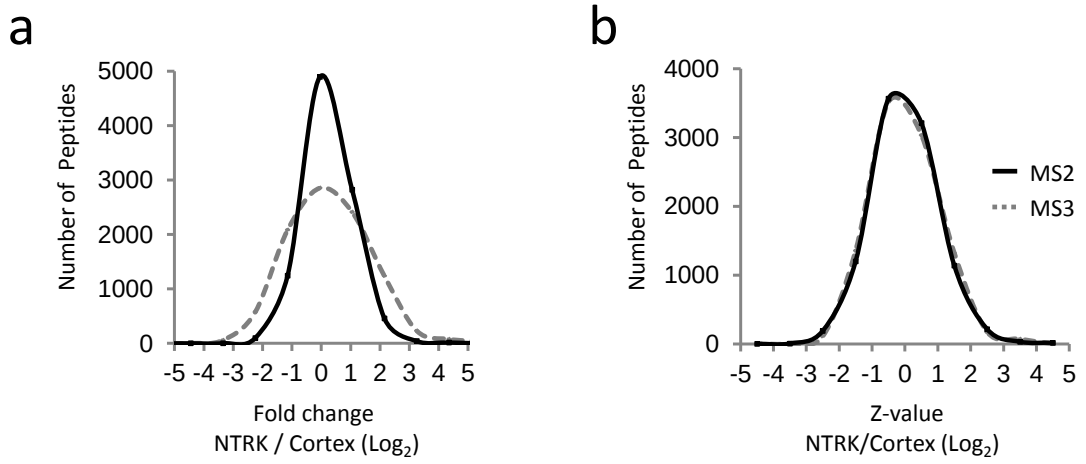

Supplementary Figure 11 | TMT-based quantification using MS2 method has essentially no impact on protein differential expression analysis after Z-scale normalization

a. Quantitative ratio compression occurred in TMT labeling strategy using MS2 compare to MS3 method. MS3 strategy can essentially eliminate ratio compression with the cost of more duty cycles and the use of low resolution MS2 data for identification, which often compromise peptide/protein identification. Comparison between MS2 and MS3 methods on the same sample using TMT labeling shows smaller difference/variance measured in MS2 method compare to MS3 method, suggesting quantitative ratio compression in MS2 analysis of TMT labeling.

b. Z scale normalization essentially eliminates the effect of ratio compression on protein differential expression analysis. Z scale transformation of the same data shows almost exact same Z value distribution in MS2 and MS3 method, suggesting similar amount of DE proteins with the same Z value cutoffs for differential expression analysis comparing MS2 and MS3 methods.